Dysregulation of Notch and ERα signaling in AhR$^{-/-}$ male mice

Bo Huang[a], Ryan Butler[a], Yifei Miao[a], Yubing Dai[a], Wanfu Wu[a], Wen Su[a], Yoshiaki Fujii-Kuriyama[b], Margaret Warner[a], and Jan-Åke Gustafsson[a,c,1]

[a]Center for Nuclear Receptors and Cell Signaling, University of Houston, Houston, TX 77204; [b]Molecular and Cellular Biosciences, University of Tokyo, Bunkyo-ku, Tokyo 113-0032, Japan; and [c]Center for Medical Innovations, Department of Biosciences and Nutrition, Karolinska Institutet, Novum 141 86, Sweden

Contributed by Jan-Åke Gustafsson, August 9, 2016 (sent for review July 31, 2016; reviewed by Christopher Bradfield and Stephen Safe)

The aryl hydrocarbon receptor (AhR) is now recognized as an important physiological regulator in the immune and reproductive systems, and in the development of the liver and vascular system. AhR regulates cell cycle, cell proliferation, and differentiation through interacting with other signaling pathways, like estrogen receptor α (ERα), androgen receptor (AR), and Notch signaling. In the present study, we investigated Notch and estrogen signaling in AhR$^{-/-}$ mice. We found low fertility with degenerative changes in the testes, germ cell apoptosis, and a reduced number of early spermatids. There was no change in aromatase, AR, ERα, or ERβ expression in the testis and no detectable change in serum estrogen levels. However, expression of Notch receptors (Notch1 and Notch3) and their target Hairy and Enhancer of Split homolog 1 (HES1) was reduced. In addition, the testosterone level was slightly reduced in the serum. In the mammary fat pad, AhR appeared to regulate estrogen signaling because, in AhR$^{-/-}$ males, there was significant growth of the mammary ducts with high expression of ERα in the ductal epithelium. The enhanced mammary ductal growth appears to be related to overexpression of ERα accompanied by a high proliferation index, whereas the reduced fertility appears to be related defects in Notch signaling that leads to reduced expression of HES1 and, consequently, early maturation of spermatocytes and a depletion of primary spermatids. Previous reports have indicated that AhR pathway is associated with infertility in men. Our results provide a mechanistic explanation for this defect.

aryl hydrocarbon receptor | low fertility | testosterone | germ cell apoptosis | mammary gland

The aryl hydrocarbon receptor (AhR) is a member of the basic helix–loop–helix PAS (Per-AhR/Arnt-Sim) family (1, 2). Upon ligand binding, the AhR translocates from the cytoplasm to the nucleus where it dimerizes with its partner Aryl Hydrocarbon Receptor Nuclear Translocator (ARNT). The AhR/ARNT heterodimer binds to its cognate DNA sequences, termed xenobiotic response elements (XREs), and activates the expression of AhR target genes, including several genes involved in xenobiotic metabolism. AhR can function as a mediator of dioxin toxicity by activating drug-metabolizing enzyme genes (3). AhR also plays important physiological functions such as in liver development, female reproduction, the immune system through regulating cell cycle, cell proliferation, cell apoptosis, cell differentiation, and inflammation (3–5). Studies have shown that AhR can interact with other signaling pathways including estrogen receptor, androgen receptor, and NF-κB signaling pathway (6–9).

Through analysis of AhR knockout (AhR$^{-/-}$) mice, it has been demonstrated that AhR plays an important role in female reproduction (10). Lack of AhR causes low fertility in AhR$^{-/-}$ female mice as a result of defects in late folliculogenesis and decreased intraovarian estrogen concentrations during preovulatory stages. The cause of the ovarian estrogen decrease is that AhR directly regulates aromatase gene (*Cyp19*) expression in ovary (10). Further evidence has suggested that AhR regulates *Cyp19* expression in cooperation with the orphan nuclear receptor, Ad4BP/SF-1 (10).

Previous studies on the role of AhR in reproduction in male mice revealed that seminal vesicles were regressed in the aged AhR$^{-/-}$ male mice (11). In the present study, we found no such regression in young or old AhR$^{-/-}$ male mice, but nonetheless fertility was reduced and there was marked growth of mammary ducts. We provide evidence that AhR regulates Notch signaling and germ cell apoptosis to control male fertility and regulates ERα expression to control growth of mammary ducts.

Results

Low Fertility of Young AhR-Deficient Male Mice with No Change of Aromatase in Testis. A previous study found that the loss of AhR causes reduced fertility in male mice and that regression of the seminal vesicles was responsible for this phenotype in the aged AhR$^{-/-}$ male mice (11). We found reduced fertility in young AhR$^{-/-}$ male mice measured by number of pups in a litter. Because we found no regression of seminal vesicles in young mice, the cause of infertility had to be further investigated. In females, AhR plays a critical role in fertility by directly regulating aromatase gene (*Cyp19*) expression (10), but in males, overexpression of *Cyp19* is associated with low fertility (12). We investigated whether the expression level of aromatase is affected by depletion of AhR in male mice. The testes of AhR$^{-/-}$ and AhR$^{+/+}$ mice were stained for aromatase with immunofluorescence and immunohistochemistry. As shown in Fig. 1*A*, there was no significant difference in aromatase expression between the testes of AhR$^{+/+}$ and AhR$^{-/-}$ mice. In addition, no significant change of *Cyp19A1* expression was detected in male mouse mammary tissue with real-time PCR (Fig. 1*B*). These results suggested that the mechanism through which AhR

Significance

The aryl hydrocarbon receptor (AhR), in addition to its well-known role in repressing ER signaling, has now been shown to have a physiological function in regulating Notch signaling. Thus, in AhR$^{-/-}$ male mice, there is growth of mammary ducts and degenerative changes in the testes. There is germ cell apoptosis, reduction of expression of Notch1 and Notch3 in Sertoli cells and slightly reduced serum testosterone level. Male infertility (affecting approximately 7% of all men) and gynecomastia (benign growth of the mammary gland in men) are two disorders for which there is need for better intervention. The study suggests that the AhR may be targeted to treat these disorders.

Author contributions: B.H., M.W., and J.-Å.G. designed research; B.H., R.B., Y.M., and M.W. performed research; Y.D., W.W., W.S., and Y.F.-K. contributed new reagents/analytic tools; B.H., M.W., and J.-Å.G. analyzed data; and B.H., M.W., and J.-Å.G. wrote the paper.

Reviewers: C.B., University of Wisconsin; and S.S., Texas A&M University.

The authors declare no conflict of interest.

[1]To whom correspondence should be addressed. Email: jgustafsson@uh.edu.

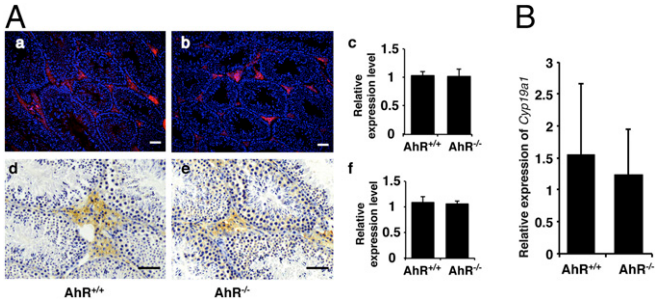

Fig. 1. AhR depletion did not affect the expression of aromatase. (*A*) Aromatase protein level remained unchanged in AhR null mouse testis. (*A*, *a* and *b*) IF staining of aromatase protein (red) in $AhR^{+/+}$ and $AhR^{-/-}$ testis. Slides have been counterstained with DAPI (blue) to mark nuclei. (*A*, *c*) Quantification of IF staining using ImageJ software showed that there is no significant difference of aromatase expression between $AhR^{+/+}$ and $AhR^{-/-}$ mice. (*A*, *d* and *e*) IHC staining of aromatase protein (brown stain) in $AhR^{+/+}$ and $AhR^{-/-}$ testis. (*A*, *f*) Quantification of IHC staining using ImageJ software showed that there is no significant difference of aromatase expression between $AhR^{+/+}$ and $AhR^{-/-}$ mice. (Scale bars: 25 μm.) (*B*) AhR depletion does not affect the expression of aromatase gene in male mouse mammary gland. Real-time PCR showed the relative expression of *Cyp19a1* in $AhR^{+/+}$ and $AhR^{-/-}$ mammary glands. The difference is not significant.

regulates female reproduction is different from that regulating male reproduction.

Giant Cells/Degenerated Spermatocytes in $AhR^{-/-}$ Testis. In the initial step of spermatogenesis, spermatogonia generate primary spermatocytes by mitosis. Because spermatogonia are the stem cells of spermatogenesis, this cell type is the first to be investigated when there is spermatogenic impairment. To determine whether there were defects in proliferation of spermatogonia, we examined expression of the proliferation marker Ki67 (Fig. 2). There was no detectable difference in proliferation between 11-wk $AhR^{+/+}$ and $AhR^{-/-}$ male testis. This result indicates that this step from spermatogonia to spermatocytes is normal in the absence of AhR.

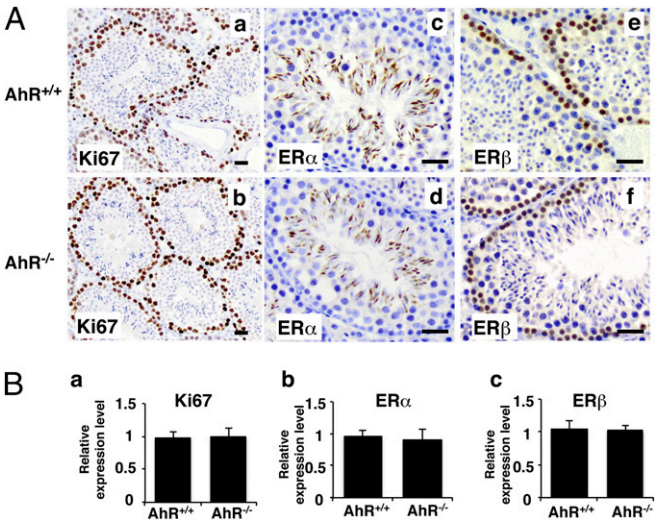

Fig. 2. Proliferation and estrogen receptors in $AhR^{-/-}$ testis. (*A*) IHC staining of Ki67 (*a* and *b*) (brown stain), ERα (*c* and *d*) (brown stain), and ERβ (*e* and *f*) (brown stain) in $AhR^{+/+}$ and $AhR^{-/-}$ testis. (Scale bars: 12.5 μm.) (*B*) Quantification of IHC staining of Ki67 (*a*), ERα (*b*), and ERβ (*c*) in $AhR^{+/+}$ and $AhR^{-/-}$ testes by using ImageJ software. Statistical analysis found that the expression of Ki67 (*B*, *a*), ERα (*B*, *b*), and ERβ (*B*, *c*) showed no significant difference between $AhR^{+/+}$ and $AhR^{-/-}$ testes.

Interestingly, despite the clear function of ERβ in preventing proliferation in many cells, the ER in spermatogonia is ERβ, not ERα. However, ERα, but not ERβ, is well expressed in late spermatids (Fig. 2). These differences in expression of the two ERs in seminiferous tubules suggest distinct functions for the two estrogen receptors in spermatogenesis.

There were more giant cells with condensed and pyknotic nuclei in some seminiferous tubules in $AhR^{-/-}$ than in $AhR^{+/+}$ male mice (Fig. 3). This type of giant cells in mouse testis could be caused by increased apoptosis in spermatocytes (13). The TUNEL assay was used to investigate whether increased apoptosis was also the cause of an increased number of giant cells in $AhR^{-/-}$ mice. As shown in Fig. 4, we found that there were more apoptotic bodies in $AhR^{-/-}$ mice than in $AhR^{+/+}$ mice, indicating that AhR regulates mouse germ cell apoptosis and, thus, regulates spermatogenesis. Because the proliferation of germ cells did not change in $AhR^{-/-}$ mice, the increased germ cell apoptosis might cause the low sperm counts in males. Low sperm count has been shown to be one of the reasons for male low fertility or infertility. Thus, germ cell apoptosis might be one factor contributing to the low fertility of $AhR^{-/-}$ male mice.

Notch Signaling Suppressed in $AhR^{-/-}$ Mouse Testicular Function. Notch signaling plays an essential role in mouse spermatogenesis (14). Blocking Notch signaling in vivo induces male germ cell fate aberrations and, significantly, increases germ cell apoptosis (14). The Notch cascade consists of Notch and Notch ligands, as well as intracellular proteins transmitting the Notch signal to the cell's nucleus. One of the main Notch effector genes is Hairy and Enhancer of Split homolog 1 (HES1). We have shown that HES1 is an AhR target gene (15). This result indicates that AhR could regulate spermatogenesis by controlling HES1 expression. To determine whether Notch signaling in the testis was affected by inactivation of AhR, we used immunohistochemistry to examine the expression of HES1, Notch1, Notch3, and Jagged 1 (JAG1), the ligand for Notch signaling receptors. As shown in Fig. 5, in $AhR^{+/+}$ mice, HES1 is expressed in spermatids, whereas in $AhR^{-/-}$ testis, HES1 expression was markedly reduced. Notch1 and Notch3 were also markedly reduced in the $AhR^{-/-}$ testis but JAG1 remained unchanged. Notch1 is predominantly expressed in Sertoli cells, whereas Notch3 is expressed abundantly in spermatocytes, spermatogonia, spermatids, and Sertoli cells. The Notch ligand, JAG1, is mostly expressed in spermatocytes but not in spermatogonia. The expression pattern of Notch signaling components indicates that the Notch pathway may mediate a crosstalk between different stages of germ cells (from spermatogonia to spermatocytes and spermatids). These results suggest that AhR controls Notch signaling by regulating the expression of Notch

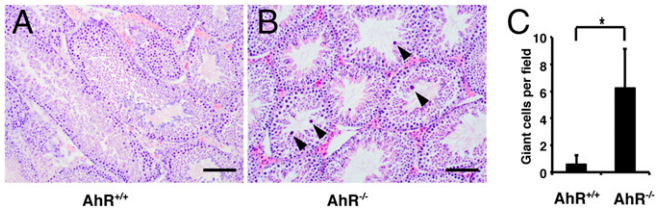

Fig. 3. Giant cells/degenerated spermatocytes in $AhR^{-/-}$ testis. (*A* and *B*) H&E staining of $AhR^{+/+}$ (*A*) and $AhR^{-/-}$ (*B*) testis. (Scale bars: 25 μm.) Note that some cells in the tubule contain condensed and pyknotic nuclei (indicated by black arrowheads). They may represent apoptotic bodies. (*C*) Graphic diagram to show the numbers of condensed and pyknotic nuclei per field by using 10× lens (*$P < 0.01$). For counting these giant cells, randomly selected stained slides from three mice in each group and more than six representative fields of each slide were counted under light microscope using 10× lens.

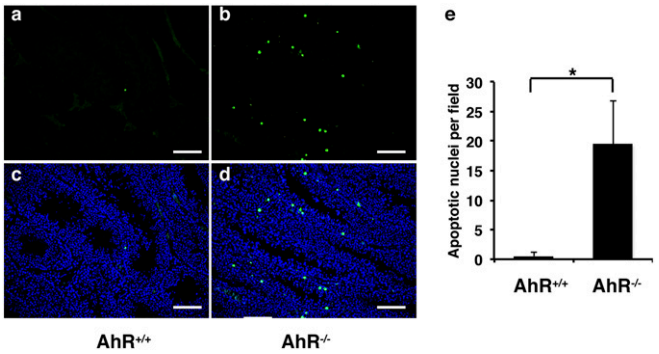

Fig. 4. TUNEL assay (green fluorescence) to show that there is increased apoptosis in AhR$^{-/-}$ mouse testis. (*A* and *C*) AhR$^{+/+}$ testis. (*B* and *D*) AhR$^{-/-}$ testis. (*E*) Graphic diagram to show the numbers of apoptotic nuclei per field by using 10× lens (*$P < 0.01$). *A* and *B*, TUNEL staining; *C* and *D*, DAPI plus TUNEL staining. For counting these apoptotic nuclei, randomly selected stained slides from three mice in each group and more than six representative fields of each slide were counted under light microscope using 10× lens.

receptors and their target effectors, but not by regulating the expression of their ligands.

Reduced Testosterone Level in AhR$^{-/-}$ Male Mice. Testosterone removal or androgen receptor (AR) inhibition induces testicular germ cell apoptosis (16–18). We measured the serum testosterone level in 11-wk mice and found a small but significant decrease in testosterone levels in AhR$^{-/-}$ mice (Fig. 6*A*). However, there was no detectable difference between AhR$^{+/+}$ and AhR$^{-/-}$ mice in the level of androgen receptor in the testis (Fig. 6*B*). This result suggests that the small decrease in testosterone, with no change in AR, is unlikely to be contributing to testicular germ cells apoptosis.

Mammary Gland Development in AhR$^{-/-}$ Male Mice. Using whole mounts of mammary fat pads with Carmine Alum staining, a well-organized ductal structure was seen in AhR$^{-/-}$ male mice (Fig. 7 *A*, *e* and *f*). We examined the male mice from 4 wk to 12 mo, and these structures were found at all ages. In 4-wk and 11-wk-old mice, there were terminal end buds (TEBs) at the tips of ducts, indicating that the ducts were actively elongating. H&E staining demonstrated these fine ductal structures (Fig. 7 *B*, *a–d*). Ki67 staining confirmed that in TEBs, proliferation was high (Fig. 7 *B*, *e*). The mammary ducts in male AhR$^{-/-}$ mice did not fill the whole mammary fat pads even in 9- and 12-mo-old mice (Fig. 7 *A*, *g* and *h*). At 9 mo, proliferation had ceased but the ducts remained (Fig. 7*B*). These mammary ducts had no tertiary structures and lacked alveolar structures. These ductal structures did not proceed to hyperplasia or tumors (Fig. 7*A*).

Expression of ERα, ERβ, and Progesterone Receptor in AhR$^{-/-}$ Mammary Glands. Mammary gland development has been reported in aromatase overexpressing transgenic male mice (19, 20). To test whether the expression of aromatase in AhR$^{-/-}$ mice also changed, we compared aromatase level in AhR$^{+/+}$ and AhR$^{-/-}$ mice. First, as shown in Fig. 1*A*, we found that the loss of AhR did not affect aromatase expression in the testis. Second, when we examined the expression level of aromatase in male mouse mammary tissue by using real-time PCR, no significant change of *Cyp19A1* expression was detected (Fig. 1*B*). Because loss of AhR did not change aromatase level in the testis, which is the primary location for converting testosterone into estrogen, or in local mammary tissue, which is an extragonadal site for estrogen biosynthesis, dysregulation of aromatase expression does not appear to be the cause of excessive ductal growth in AhR$^{-/-}$ male mice. Using immunohistochemistry, we studied the expression of ERα, ERβ, and progesterone receptor (PR) in the female and male mammary glands. We found that expression of ERα was higher in both female and male AhR$^{-/-}$ mouse mammary gland over the respective WT littermates (Fig. 8 *A*, *a–c*), whereas ERβ and PR expression was not changed (Fig. 8 *A*, *d–i*).

Discussion

In the present study, we found mechanisms for AhR in regulating male reproduction. In the testes of AhR$^{-/-}$ mice there were multinucleated giant cells, a sign of a degenerative syndrome. Giant cells represent abnormal progenies of the tetraploid primary spermatocytes that do not complete their meiotic division but nevertheless retain their normal capacity to progress to the seminiferous lumen (21). Further experiments illustrated that depletion of AhR induced germ cell apoptosis. This result is similar to the finding from another report, which used a different strategy to knock out AhR in mice (22). Along with infertility in this study, we found ductal growth in the mammary fat pad of male AhR$^{-/-}$ mice. We further discovered that AhR depletion resulted in increased expression of ERα in ductal epithelium and increased proliferation. All of these findings indicate that AhR plays an important role in the regulation of male reproduction and mammary gland development.

There are several pathways that lead to germ cell apoptosis (17). Among them, testosterone removal or AR inhibition have been shown to play critical roles in controlling testicular germ cell apoptosis (16–18). Using immunohistochemistry, we found no difference in AR expression in the testis of AhR$^{-/-}$ vs. AhR$^{+/+}$ mice (Fig. 6). However, we found that loss of AhR caused a decrease in testosterone in male mice (Fig. 6). A previous study found that in female mice, AhR controls the conversion of testosterone to estradiol by directly regulating aromatase expression (10). However, unlike the function in female mice, AhR did not regulate aromatase expression in male mice (Fig. 1).

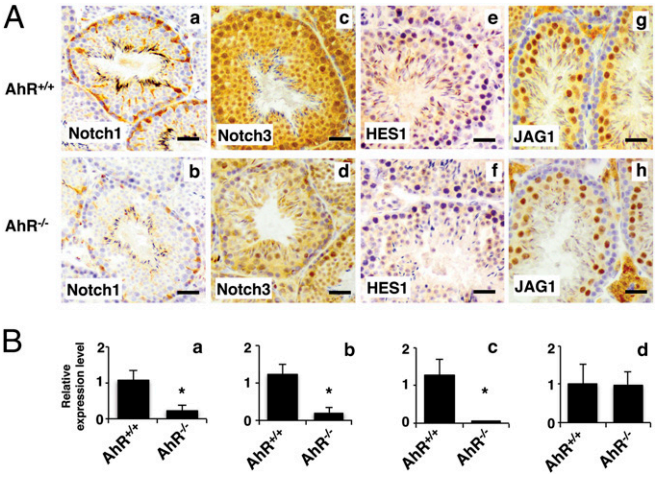

Fig. 5. AhR depletion affected Notch signaling pathway. (*A*). IHC staining (brown stain) of Notch1 (*a* and *b*), Notch3 (*c* and *d*), HES1 (*e* and *f*), and JAG1 (*g* and *h*) in AhR$^{+/+}$ and AhR$^{-/-}$ testes. (Scale bars: 12.5 μm). Notch 1 in surface of Sertoli cells, Notch 3 in nuclei of spermatogonia and all subsequent daughter cells, HES1 in primary spermatids, JAG1 exclusively in primary spermatocytes but not in spermatogonia. JAG1 is not changed in AhR$^{-/-}$ mice. Notch 1, Notch 3, and HES1 are lost in AhR$^{-/-}$ mice. (*B*) Quantification of IHC staining of Notch1 (*a*), Notch3 (*b*), HES1 (*c*), and JAG1 (*d*) in AhR$^{+/+}$ and AhR$^{-/-}$ testes using ImageJ software. Statistical analysis found that the expression of Notch1, Notch3, and HES1 showed significant difference between AhR$^{+/+}$ and AhR$^{-/-}$ testes (*$P < 0.01$), whereas the expression of JAG1 showed no significant difference between AhR$^{+/+}$ and AhR$^{-/-}$ testes.

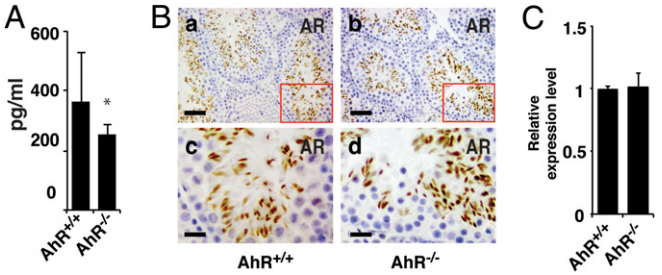

Fig. 6. The level of testosterone in AhR$^{-/-}$ male mice was significantly reduced, whereas loss of AhR did not alter the expression of AR in testis. (*A*) Testosterone level in AhR$^{+/+}$ and AhR$^{-/-}$ serum measured by ELISA kit. (*B*) IHC staining of AR in AhR$^{+/+}$ (*a* and *c*) and AhR$^{-/-}$ (*b* and *d*) testis; *c* and *d* are in high magnification to show the staining details. (Scale bars: *a* and *b*, 25 μm; *c* and *d*, 8.3 μm.) (*C*) Quantification of IHC staining of AR in AhR$^{+/+}$ and AhR$^{-/-}$ testes using ImageJ software. Statistical analysis found that the expression of AR showed no significant difference between AhR$^{+/+}$ and AhR$^{-/-}$ testes.

The Notch signaling pathway is a ligand- and receptor-based signaling pathway mediating communication between adjacent cells. Upon ligand binding to a receptor, the intracellular domain of the receptor is released from the plasma membrane and translocates into the nucleus, where it can activate its target gene expression (23). Blockade of Notch signaling has been shown to induce male germ cell fate aberrations, and significantly increase germ cell apoptosis (14). In the present study, we found that the expression of Notch receptors Notch1 and Notch3 and their target effector HES1 were markedly reduced in AhR$^{-/-}$ mouse testis (Fig. 5). These results suggested a mechanism for which AhR in regulating male fertility might be controlling Notch signaling pathway. Because *Hes1* is the direct target gene of AhR (15), there were two possible routes through which AhR could execute its function in testis development and spermatogenesis: (*i*) AhR controlling Notch receptor Notch3 and then indirectly regulating Notch signaling target HES1; and (*ii*) AhR directly controlling *Hes1* mRNA level in testis.

In adult males, reduction in testosterone levels leads to changes in mood, muscle function, function of the testis, and gynecomastia (enlarged breasts in men). In the present study, we discovered abnormal mammary gland ductal development in AhR$^{-/-}$ male mice. The AhR$^{-/-}$ mouse thus is a model for studying human gynecomastia, which is more a social and psychological problem than a health hazard but it is also a risk factor for male breast cancer (24). Male transgenic mice overexpressing aromatase also develop mammary gland-like structures (19, 20). There are two lines of aromatase transgenic mice. In one (MMTV-arom^{+}), the aromatase cDNA was expressed under the control of mouse mammary tumor virus promoter, which is active in male reproductive organs and in mammary tissues (20). Another line (AROM^{+}) was generated by expressing human aromatase cDNA under the control of the ubiquitin C promoter (19). AhR$^{-/-}$ mice and the above two aromatase-overexpressing lines all develop well-organized ductal structures. However, AhR$^{-/-}$ mice did not develop lobuloalveolar structures, which are present in the two aromatase-overexpressing lines. Mammary glands in aromatase overexpressing male mice develop either gestation-like phenotype (19) or hyperplasia (20), whereas AhR$^{-/-}$ male mice do not. The differences might be caused by the fact that in AhR$^{-/-}$ male mice, the aromatase expression level was not changed. Because there are no lobular structures in human gynecomastia (24), the AhR$^{-/-}$ mouse may be a better model for human gynecomastia than the AROM^{+} mouse.

Disruption of AhR has also been reported to affect mammary gland development in female mice (25). In this report, the authors found that targeted gene inactivation of AhR results in a decrease in TEBs and increase in blunt-ended terminal ducts during postnatal development (25). In female AhR$^{-/-}$ mice, the decline of aromatase gene (*Cyp19*) level resulted in the decrease of the ovarian estrogen (10). Because estrogen plays an essential role in controlling female mammary gland postnatal development (26, 27), the reported TEBs phenotype in female AhR$^{-/-}$ mice might be caused by the decrease of the ovarian estrogen, which was regulated by the AhR target gene *Cyp19*. However, in male mice, there were no significant differences of estrogen and the enzyme aromatase levels between AhR$^{+/+}$ and AhR$^{-/-}$ mice (Fig. 1). It seems that estrogen itself cannot explain the gynecomastia in male AhR$^{-/-}$ mice. The action of hormones needs to be executed by their receptors. In the mammary gland development, both hormones (estrogen, progesterone) and hormone receptors (ERs, PR) are critical (27). Interplay between AhR and ER signaling pathways has been reported to play an important role in ERα signaling (7). To test whether AhR could regulate these hormone receptors, we studied the expression of ERα, ERβ, and PR in mouse mammary gland. We found that ERα level increased markedly in AhR$^{-/-}$ female and male mammary glands, whereas ERβ and PR levels were not significantly changed (Fig. 8). Because ERα regulates mammary gland ductal elongation/bifurcation (27), whereas ERβ and PR regulate side branching and alveologenesis (27–29), the increased ERα expression could be the cause of the ductal structures in AhR$^{-/-}$ male mice.

Despite the role in the mammary gland, in the testes, the ERα level in germ cells is not regulated by Ah receptor (Fig. 2). ERα was mostly expressed in elongated spermatids, whereas ERβ was mainly expressed in spermatogonia. The presence of ERβ in highly proliferative spermatogonial cells (Fig. 2 and refs. 30 and 31) indicates that in these cells, ERβ does not inhibit cell proliferation. The finding is interesting because it adds a dimension to the role of ERβ in cell proliferation (i.e., ERβ does not always inhibit cell proliferation as previously thought).

In conclusion, the AhR pathway is much more that a xenobiotic metabolism-inducing pathway, and the regulation by AhR of Notch signaling in the testis offers some insight into the mechanism of infertility in men.

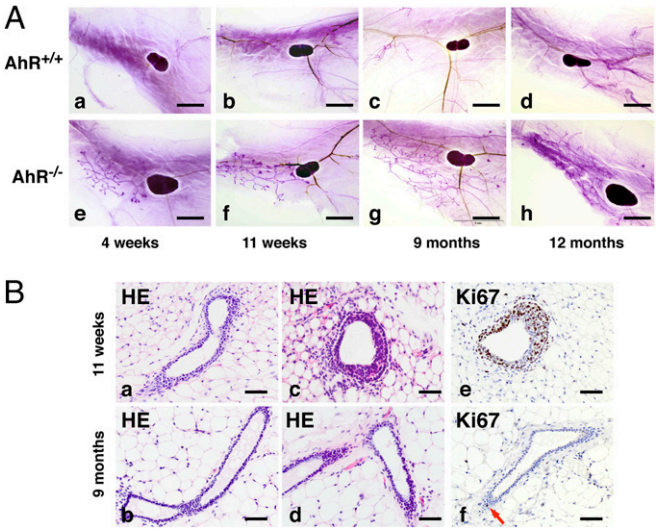

Fig. 7. AhR depletion causes development of mammary glands in male mice. (*A*) Whole-mount analysis of male fat pad from AhR$^{-/-}$ and control AhR$^{+/+}$ mice. The fat pads were taken from AhR$^{+/+}$ mice (*a*, 4 wk; *b*, 11 wk; *c*, 9 mo; and *d*, 12 mo) or AhR$^{-/-}$ mice (*e*, 4 wk; *f*, 11 wk; *g*, 9 mo; and *h*, 12 mo) and were stained with carmine alum (see *Materials and Methods* for details). The lymph node serves as a reference point to evaluate ductal growth. (*B*) H&E (*a*–*d*) and Ki67 (brown stain) (*e* and *f*) staining for mammary gland from male AhR$^{-/-}$ mice. (Scale bars: *A*, 2.5 mm; *B*, 25 μm.)

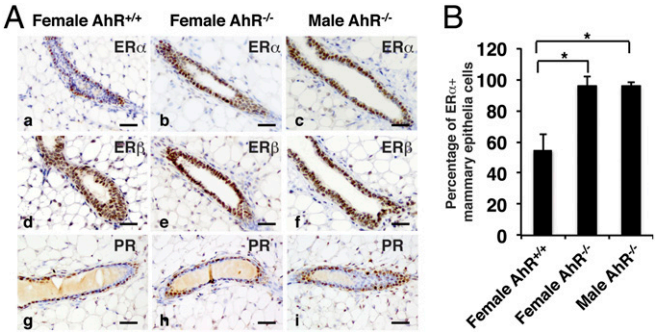

Fig. 8. AhR depletion increases expression of ERα in mouse mammary glands. (*A*) IHC staining of ERα (*a–c*), ERβ (*d–f*), and PR (*g–i*) in female $AhR^{+/+}$ (*a*, *d*, and *g*), female $AhR^{-/-}$ (*b*, *e*, and *h*), and male $AhR^{-/-}$ (*c*, *f*, and *i*) mammary glands. (Scale bars: 25 μm.) Brown staining indicates ERα, ERβ, and PR. Slides have been counterstained with hematoxylin (blue nuclear staining). (*B*) Quantification of IHC staining to show the percentage of $ER\alpha^+$ mammary epithelia cells in ducts from female $AhR^{+/+}$, female $AhR^{-/-}$, and male $AhR^{-/-}$ mammary glands (*$P < 0.05$). Total and $ER\alpha^+$ mammary epithelia cells in each slide were counted by using ImageJ software. The quotient obtained by dividing $ER\alpha^+$ mammary epithelia cells by total mammary epithelia cells was calculated as the percentage of $ER\alpha^+$ mammary epithelial cells.

Materials and Methods

Mice. AhR knockout mice were generated in the Y.F.-K. laboratory by using a homologous recombination as described (32). All animal experiments were approved by the Institutional Animal Care and Use Committee at the University of Houston. The $AhR^{+/-}$ mice were interbred to yield $AhR^{+/+}$, $AhR^{+/-}$, and $AhR^{-/-}$ mice. Genotyping was done by using PCR method as described previously (33). Five animals for each age group were used in the experiment. All experiments use 11-wk-old mice, unless otherwise noted.

Morphological and Histological Assessment of Testes and Mammary Glands. Mouse testes were removed and fixed in 4% (wt/vol) paraformaldehyde (PFA) overnight at 4 °C. Then the tissues were embedded in paraffin, sectioned at 5 μm, and stained with hematoxylin and eosin (H&E). The fourth inguinal mammary glands were removed from $AhR^{-/-}$ mice and age-matched $AhR^{+/+}$ mice. Mammary gland whole mounts were prepared as described (34). Briefly, the mammary gland was excised from the mouse and spread directly on a glass slide. The gland was fixed in Carnoy's fixative (100% EtOH, chloroform, glacial acetic acid; 6:3:1) at 4 °C overnight. After fixation, stained mammary glands were placed in carmine alum for 2 d at room temperature. The carmine alum was removed, and the stained tissues were gradually dehydrated through serial ethanol baths and cleared in xylene. Mammary glands were then mounted in Permount, and pictures were taken under the dissecting microscope. Routine section of mammary glands were prepared after fixation with 4% (wt/vol) PFA and stained with H&E.

Real-Time PCR. Real-time PCR was performed to assess the expression of *Cyp19A1* gene. Total mRNA was extracted from mouse inguinal mammary glands by using RNeasy Lipid Tissue Mini Kit (Qiagen). cDNA synthesis and PCR conditions were described (35). Primers for the mouse *Cyp19A1* gene were 5′-AAATGCTGAACCCCATGCAG-3′ and 5′-AATCAGGAGAAGGAGGCCCAT-3′ as used (36). GAPDH, a housekeeping gene, was used as the internal control.

Immunohistochemistry and Immunofluorescence. Immunohistochemistry was performed as described (37). Antibodies used were anti-aromatase (1:200, NBP1-19697; Novus Biologics), anti-Ki67 (1:500, ab15580; Abcam), anti-Notch1 (1:400, ab52627; Abcam), anti-Notch3 (1:400, ab23426; Abcam), anti-ERα (1:200, ab75635; Abcam), anti-ERβ (503 IgY; homemade), anti-PR (1:400, sc-538; Santa Cruz Biotechnology), and anti-JAG1 (1:400, sc-6011; Santa Cruz Biotechnology). Second antibody for immunofluorescence was Alexa Fluor 594 donkey anti-rabbit IgG (H+L) antibody (Lifescience Technology). For ERβ IHC staining, the second antibody was the biotinylated goat anti-chicken IgY antibody (Abcam); for Ki67 IHC staining, the second antibody was the biotinylated goat anti-mouse IgG antibody (Invitrogen); for ERα, PR, Notch1, Notch3, and aromatase, the second antibody was the biotinylated goat anti-rabbit IgG antibody (Invitrogen); for JAG1, the second antibody was the biotinylated donkey anti-goat IgG antibody (Abcam).

TUNEL Assay. TUNEL assay was done by using In Situ Cell Death Detection Kit, Fluorescein (catalog no. 11684795910; Roche), according to manufacturer's recommendation with some modifications. Briefly, slides were dewaxed and rehydrated and were then incubated with Proteinase K working solution for 20 min at room temperature. After washing with PBS, slides were incubated with TUNEL reaction mixture for 1 h at 37 °C. Slides were rinsed three times with PBS and analyzed under a fluorescence microscope.

Hormone Level Detection. Five $AhR^{+/+}$ and five $AhR^{-/-}$ male mice at age of 11 wk were used to measure serum testosterone level by using testosterone high sensitivity ELISA kit (Enzo Life Sciences; catalog no. ADI-900-176). The procedure is briefly described below: (*i*) Samples were extracted from serum by the Solid Phase Extraction method using 200 mg of C_{18} solid phase system columns; (*ii*) samples were incubated with conjugation solution and antibody at room temperature with shaking (~500 rpm) for 2 h; (*ii*) after washing three times with wash buffer, 200 μL of the substrate solution was added into each well and incubated for 1 h at room temperature with shaking; (*iv*) the stop solution was added into each well and the optical density was read at 405 nm after blanking the plate reader against the substrate blank; and (*v*) the concentration was calculated by using an Excel spreadsheet.

Quantification of Histological Staining Using ImageJ. For the quantification of immunohistochemistry (IHC)/immunofluorescence (IF) staining, randomly selected stained slides from three mice in each group and more than six representative fields of each slide were analyzed by National Institutes of Health (NIH) ImageJ software according to ref. 38. The positive staining in each slide was scored and presented as the relative expression level (the protein expression level in $AhR^{+/+}$ mice was arbitrarily set to base level of 1). Data were expressed as mean ± SD.

Statistical Analysis. All statistical analyses were performed by using SPSS 22 (SPSS), and $P < 0.05$ was deemed to indicate statistical significance.

ACKNOWLEDGMENTS. This work was supported by Robert A. Welch Foundation Grant E-0004, the Swedish Science Council, and the Center for Medical Innovations.

1. Ema M, et al. (1992) cDNA cloning and structure of mouse putative Ah receptor. *Biochem Biophys Res Commun* 184(1):246–253.
2. Burbach KM, Poland A, Bradfield CA (1992) Cloning of the Ah-receptor cDNA reveals a distinctive ligand-activated transcription factor. *Proc Natl Acad Sci USA* 89(17):8185–8189.
3. Bock KW, Köhle C (2009) The mammalian aryl hydrocarbon (Ah) receptor: From mediator of dioxin toxicity toward physiological functions in skin and liver. *Biol Chem* 390(12):1225–1235.
4. Stevens EA, Mezrich JD, Bradfield CA (2009) The aryl hydrocarbon receptor: A perspective on potential roles in the immune system. *Immunology* 127(3):299–311.
5. Gonzalez FJ, Fernandez-Salguero P (1998) The aryl hydrocarbon receptor: Studies using the AHR-null mice. *Drug Metab Dispos* 26(12):1194–1198.
6. Khan S, et al. (2006) Molecular mechanism of inhibitory aryl hydrocarbon receptor-estrogen receptor/Sp1 cross talk in breast cancer cells. *Mol Endocrinol* 20(9):2199–2214.
7. Matthews J, Gustafsson JA (2006) Estrogen receptor and aryl hydrocarbon receptor signaling pathways. *Nucl Recept Signal* 4:e016.
8. Vogel CF, et al. (2014) Cross-talk between aryl hydrocarbon receptor and the inflammatory response: A role for nuclear factor-κB. *J Biol Chem* 289(3):1866–1875.
9. Wu Y, Baumgarten SC, Zhou P, Stocco C (2013) Testosterone-dependent interaction between androgen receptor and aryl hydrocarbon receptor induces liver receptor homolog 1 expression in rat granulosa cells. *Mol Cell Biol* 33(15):2817–2828.
10. Baba T, et al. (2005) Intrinsic function of the aryl hydrocarbon (dioxin) receptor as a key factor in female reproduction. *Mol Cell Biol* 25(22):10040–10051.
11. Baba T, et al. (2008) Disruption of aryl hydrocarbon receptor (AhR) induces regression of the seminal vesicle in aged male mice. *Sex Dev* 2(1):1–11.
12. Li X, et al. (2006) Transgenic mice expressing p450 aromatase as a model for male infertility associated with chronic inflammation in the testis. *Endocrinology* 147(3):1271–1277.
13. Liu D, et al. (1998) Cyclin A1 is required for meiosis in the male mouse. *Nat Genet* 20(4):377–380.
14. Murta D, et al. (2014) In vivo notch signaling blockade induces abnormal spermatogenesis in the mouse. *PLoS One* 9(11):e113365.
15. Thomsen JS, Kietz S, Ström A, Gustafsson JA (2004) HES-1, a novel target gene for the aryl hydrocarbon receptor. *Mol Pharmacol* 65(1):165–171.
16. Sofikitis N, et al. (2008) Hormonal regulation of spermatogenesis and spermiogenesis. *J Steroid Biochem Mol Biol* 109(3-5):323–330.

DEVELOPMENTAL BIOLOGY

17. Shaha C, Tripathi R, Mishra DP (2010) Male germ cell apoptosis: Regulation and biology. *Philos Trans R Soc Lond B Biol Sci* 365(1546):1501–1515.
18. Kim JM, Ghosh SR, Weil AC, Zirkin BR (2001) Caspase-3 and caspase-activated deoxyribonuclease are associated with testicular germ cell apoptosis resulting from reduced intratesticular testosterone. *Endocrinology* 142(9):3809–3816.
19. Li X, et al. (2002) Mammary gland development in transgenic male mice expressing human P450 aromatase. *Endocrinology* 143(10):4074–4083.
20. Gill K, Kirma N, Tekmal RR (2001) Overexpression of aromatase in transgenic male mice results in the induction of gynecomastia and other biochemical changes in mammary glands. *J Steroid Biochem Mol Biol* 77(1):13–18.
21. Rotter V, et al. (1993) Mice with reduced levels of p53 protein exhibit the testicular giant-cell degenerative syndrome. *Proc Natl Acad Sci USA* 90(19):9075–9079.
22. Hansen DA, Esakky P, Drury A, Lamb L, Moley KH (2014) The aryl hydrocarbon receptor is important for proper seminiferous tubule architecture and sperm development in mice. *Biol Reprod* 90(1):8.
23. Andersson ER, Sandberg R, Lendahl U (2011) Notch signaling: Simplicity in design, versatility in function. *Development* 138(17):3593–3612.
24. Al Qassabi SS, Al-Harthi SM, Al-Osali ME (2015) Mixed gynecomastia. *Saudi Med J* 36(9):1115–1117.
25. Hushka LJ, Williams JS, Greenlee WF (1998) Characterization of 2,3,7,8-tetrachlorodibenzofuran-dependent suppression and AH receptor pathway gene expression in the developing mouse mammary gland. *Toxicol Appl Pharmacol* 152(1): 200–210.
26. Sternlicht MD, Kouros-Mehr H, Lu P, Werb Z (2006) Hormonal and local control of mammary branching morphogenesis. *Differentiation* 74(7):365–381.
27. Brisken C, O'Malley B (2010) Hormone action in the mammary gland. *Cold Spring Harb Perspect Biol* 2(12):a003178.
28. Antal MC, Krust A, Chambon P, Mark M (2008) Sterility and absence of histopathological defects in nonreproductive organs of a mouse ERbeta-null mutant. *Proc Natl Acad Sci USA* 105(7):2433–2438.
29. Förster C, et al. (2002) Involvement of estrogen receptor beta in terminal differentiation of mammary gland epithelium. *Proc Natl Acad Sci USA* 99(24):15578–15583.
30. Zhou Q, et al. (2002) Localization of androgen and estrogen receptors in adult male mouse reproductive tract. *J Androl* 23(6):870–881.
31. Mäkinen S, et al. (2001) Localization of oestrogen receptors alpha and beta in human testis. *Mol Hum Reprod* 7(6):497–503.
32. Mimura J, et al. (1997) Loss of teratogenic response to 2,3,7,8-tetrachlorodibenzo-p-dioxin (TCDD) in mice lacking the Ah (dioxin) receptor. *Genes Cells* 2(10):645–654.
33. Shimizu Y, et al. (2000) Benzo[a]pyrene carcinogenicity is lost in mice lacking the aryl hydrocarbon receptor. *Proc Natl Acad Sci USA* 97(2):779–782.
34. Plante I, Stewart MK, Laird DW (2011) Evaluation of mammary gland development and function in mouse models. *J Vis Exp* (53):2828.
35. Huang B, et al. (2012) RUNX3 acts as a tumor suppressor in breast cancer by targeting estrogen receptor α. *Oncogene* 31(4):527–534.
36. Jeong JH, et al. (2010) The gene for aromatase, a rate-limiting enzyme for local estrogen biosynthesis, is a downstream target gene of Runx2 in skeletal tissues. *Mol Cell Biol* 30(10):2365–2375.
37. Huang B, et al. (2014) Differential expression of estrogen receptor α, β1, and β2 in lobular and ductal breast cancer. *Proc Natl Acad Sci USA* 111(5):1933–1938.
38. Jensen EC (2013) Quantitative analysis of histological staining and fluorescence using ImageJ. *Anat Rec (Hoboken)* 296(3):378–381.